

Dynamic Interleaving of Content and Structure for Robust Indexing of Semi-Structured Hierarchical Data

Kevin Wellenzohn
University of Zurich

wellenzohn@ifi.uzh.ch

Michael H. Böhlen
University of Zurich

boehlen@ifi.uzh.ch

Sven Helmer
University of Zurich

helmer@ifi.uzh.ch

ABSTRACT

We propose a robust index for semi-structured hierarchical data that supports content-and-structure (CAS) queries specified by path and value predicates. At the heart of our approach is a novel dynamic interleaving scheme that merges the path and value dimensions of composite keys in a balanced way. We store these keys in our trie-based Robust Content-And-Structure index, which efficiently supports a wide range of CAS queries, including queries with wildcards and descendant axes. Additionally, we show important properties of our scheme, such as robustness against varying selectivities, and demonstrate improvements of up to two orders of magnitude over existing approaches in our experimental evaluation.

PVLDB Reference Format:

Kevin Wellenzohn, Michael H. Böhlen, Sven Helmer. Dynamic Interleaving of Content and Structure for Robust Indexing of Semi-Structured Hierarchical Data. *PVLDB*, 13(10): 1641-1653, 2020.

DOI: <https://doi.org/10.14778/3401960.3401963>

1. INTRODUCTION

A lot of the data in business and engineering applications is semi-structured and inherently hierarchical. Typical examples are bills of materials (BOMs) [7], enterprise asset hierarchies [11], and enterprise resource planning applications [12]. A common type of queries on such data are content-and-structure (CAS) queries [25], containing a *value predicate* on the *content* of some attribute and a *path predicate* on the location of this attribute in the *hierarchical structure*.

As real-world BOMs grow to tens of millions of nodes [11], we need dedicated CAS access methods to support the efficient processing of CAS queries. Existing CAS indexes often lead to large intermediate results, since they either build separate indexes for, respectively, content and structure [25] or prioritize one dimension over the other (i.e., content over structure or vice versa) [2, 8, 39]. We propose a *well-balanced integration* of paths and values in a single index that provides *robust* performance for CAS queries, meaning that the index prioritizes neither paths nor values.

We achieve the balanced integration of the path and value dimension with composite keys that *interleave* the bytes of a path and a

value. Interleaving is a well-known technique applied to multidimensional keys, for instance Nishimura et al. look at a family of bit-merging functions [31] that include the *c-order* [31] and the *z-order* [29, 33] space-filling curves. Applying space-filling curves on paths and values is subtle, though, and can result in poor query performance because of varying key length, different domain sizes, and the skew of the data. The *z-order* curve, for example, produces a poorly balanced partitioning of the data if the data contains long common prefixes [24]. The paths in a hierarchical structure exhibit this property: they have, by their very nature, long common prefixes. The issue with common prefixes is that they do not help to partition the data, since they are the same for all data items. However, the first byte following a longest common prefix does exactly this: it distinguishes different data items. We call such a byte a *discriminative byte*. The distribution of discriminative path and value bytes in an interleaved key determines the order in which an index partitions the data and, consequently, how efficiently queries can be evaluated. The *z-order* of a composite key often clusters the discriminative path and value bytes, instead of interleaving them. This leads to one dimension—the one whose discriminative bytes appear first—to be prioritized over the other, precluding robust query performance.

We develop a *dynamic interleaving* scheme that interleaves the discriminative bytes of paths and values in an alternating way. This leads to a well-balanced partitioning of the data with a robust query performance. Our dynamic interleaving is *data-driven* since the positions of the discriminative bytes depend on the distribution of the data. We use the dynamic interleaving to define the *Robust Content-and-Structure (RCAS)* index for semi-structured hierarchical data. We build our RCAS index as an in-memory trie data-structure [21] to efficiently support the basic search methods for CAS queries: *range searches* and *prefix searches*. Range searches enable value predicates that are expressed as a value range and prefix searches allow for path predicates that contain wildcards and descendant axes. Crucially, tries in combination with dynamically interleaved keys allow us to efficiently evaluate path and value predicates simultaneously. We provide an efficient bulk-loading algorithm for RCAS that scales linearly with the size of the dataset. Incremental insertions and deletions are not supported.

Our main contributions can be summarized as follows:

- We develop a *dynamic interleaving* scheme to interleave paths and values in an alternating way using the concept of *discriminative bytes*. We show how to compute this interleaving by partitioning the data. We prove that our dynamic interleaving is robust against varying selectivities (Section 5).
- We propose the in-memory, trie-based *Robust Content-and-Structure (RCAS)* index for semi-structured hierarchical data.

This work is licensed under the Creative Commons Attribution-NonCommercial-NoDerivatives 4.0 International License. To view a copy of this license, visit <http://creativecommons.org/licenses/by-nc-nd/4.0/>. For any use beyond those covered by this license, obtain permission by emailing info@vldb.org. Copyright is held by the owner/author(s). Publication rights licensed to the VLDB Endowment.

Proceedings of the VLDB Endowment, Vol. 13, No. 10
ISSN 2150-8097.
DOI: <https://doi.org/10.14778/3401960.3401963>

The RCAS achieves its robust query performance by a well-balanced integration of paths and values via our dynamic interleaving scheme (Section 6).

- Our RCAS index supports a broad spectrum of CAS queries that include wildcards and the descendant axis. We show how to evaluate CAS queries through a combination of range and prefix searches on the trie-based structure of the RCAS index (Section 6.4).
- An exhaustive experimental evaluation with real-world and synthetic datasets shows that RCAS delivers robust query performance. We get improvements of up to two orders of magnitude over existing approaches (Section 7).

2. RUNNING EXAMPLE

We consider a company that stores the bills of materials (BOMs) of its products. BOMs represent the hierarchical assembly of components to final products. Each BOM node is stored as a tuple in a relational table, which is common for hierarchies, see, e.g., SAP’s storage of BOMs [7, 11, 12] and the Software Heritage Archive [10, 34]. A CAS index is used to efficiently answer queries on the structure (location of a node in the hierarchy) and the content of an attribute (e.g., the weight or capacity). The paths of all nodes in the BOM that have a value for the indexed attribute as well as the value itself are indexed in the CAS index. The index is read-only, updated offline, and kept in main memory.

Figure 1 shows the hierarchical representation of a BOM for three products. The components of each product are organized under an `item` node. Components can have attributes to record additional information, e.g., the weight of a battery. Attributes are represented by special nodes that are prefixed with an `@` and that have an additional value. For example, the weight of the rightmost battery is 250’714 grams and its capacity is 80000 Wh.

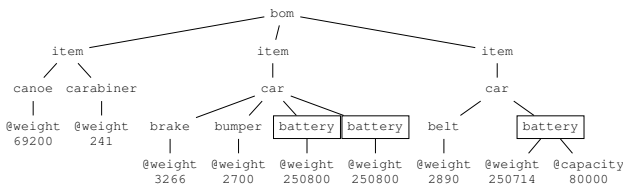


Figure 1: Example of a bill of materials (BOM).

Next, we look at an example CAS query. We roughly follow the syntax of query languages for semistructured data, such as XQuery [19] or JSONiq [14], utilizing simple FLWOR expressions.

Example 1. To reduce the weight of cars we look for all heavy car parts, i.e., parts weighing at least 50 kilograms (“`//`” matches a node and all its descendants in a hierarchical structure):

```
Q: for $c in /bom/item/car//  
  where $c/@weight >= 50000  
  return $c
```

The answer to query Q are the three framed nodes in Figure 1. Our goal is an index that guides us as quickly as possible to these nodes. Indexes on either paths or values do not perform well. An index built for only the values of weight nodes also accesses the node for the canoe. A purely structural index for the paths additionally has to look at the weight of other car parts. Our RCAS index considers values and paths together to get a good query performance.

3. RELATED WORK

We begin with a review of existing CAS indexes [8, 20, 23, 25, 39]. IndexFabric [8] prioritizes the structure of the data over its values. It stores the concatenated path and value of a key in a disk-optimized PATRICIA trie [28] that supports incremental updates (i.e., inserts and deletes). IndexFabric does not offer robust CAS query performance since a CAS query must fully evaluate a query’s path predicate before it can evaluate its value predicate. This leads to large intermediate results if the path predicate is not selective.

The hierarchical database system Apache Jackrabbit Oak [2] implements a CAS index that prioritizes values over paths. Oak indexes (value v , path p)-pairs in a DataGuide-like index that supports updates. For each value v , Oak stores a DataGuide [15] of all paths p that have this particular value v . Query performance is poor if the value predicate is not selective because the system must search many DataGuides.

The CAS index of Microsoft Azure’s DocumentDB (now Cosmos DB) concatenates paths and values [39] and stores the result in a Bw-tree [22] that supports updates. Depending on the expected query type(s) (point or range queries), the system either stores forward keys (e.g., `/a/b/c`) or reverse keys (e.g., `c/b/a`). To reduce the space requirements, forward and reverse keys are split into trigrams (three consecutive node labels). During the evaluation of a CAS query these trigrams must be joined and matched against the query, which is slow. Moreover, choosing forward or reverse keys prioritizes structure over values or vice-versa.

Mathis et al. [25] propose a CAS index that consists of two index structures: a B-tree to index the values and a structural summary (e.g., a DataGuide [15]) to index the structure of the data. The DataGuide assigns an identifier (termed PCR) to each distinct path in the documents. The B-tree stores the values along with the PCRs. The path and value predicates of a CAS query are independently evaluated on the DataGuide and the B-tree, and the intermediate results are joined on the PCR. This is expensive if the intermediate results are large (i.e., at least one predicate is not selective) but the final result is small. Updates are supported and are executed on the B-tree as well as the DataGuide.

Kaushik et al. [20] present an approach that joins inverted lists for answering CAS queries. They use a 1-index [26] to evaluate path predicates and B-trees to evaluate value predicates. This approach evaluates both predicates independently and exhibits the same problems as [25]. Updates are not discussed.

FLUX [23] computes a Bloom filter for each path into which its labels are hashed and stores these Bloom filters along with the values in a B-tree. Query evaluation proceeds as follows. The value predicate is matched on the B-tree and for each matched value the corresponding Bloom filter C is compared to a Bloom filter Q built for the query path. If each bit that is set in Q is also set in C , the path is a possible match that needs to be double-checked through database accesses. Value predicates that are not selective produce large intermediate results. Updates are not discussed.

Some document databases for semi-structured, hierarchical data (MongoDB [27], CouchDB [9], and AsterixDB [1]) use pure value indexes (e.g., standard B-trees) that index the content of documents but not their structure. They create an index on a predefined path (e.g., `/person/name`) and only index the corresponding values. They cannot answer CAS queries with arbitrary path predicates.

Besides pure value indexes there are also pure structure indexes that focus on complex twig queries with different axes (ancestor, descendant, sibling, etc.). DeltaNI [11] and Order Indexes [13] are recent proposals in this area. Pure structure indexes cannot efficiently answer CAS queries that also include value predicates.

Our RCAS index integrates paths and values by interleaving them. This is similar to the bit-merging family of space-filling curves that combine the binary representation of a key's dimensions. We compare our approach to two representatives: the *c*-order curve [31] and the *z*-order curve [29, 33]. The *c*-order curve is obtained by concatenating dimensions, which prioritizes one of the dimensions. The selectivity of the predicate on the prioritized dimension determines the query performance. If it is high and the other selectivity is low, the *c*-order curve performs badly. The *z*-order curve is a space-filling curve that is used, among others, by UB-trees [35] and k-d tries [30, 33, 36]. It is obtained by the bitwise interleaving of dimensions. The *z*-order curve produces an unbalanced partitioning of the data with poor query performance if the data contains long common prefixes. Markl calls this the “puff-pastry effect” [24] because the query performance deteriorates to that of a *c*-order curve that fully orders one dimension after another. The Variable UB-tree [24] uses a pre-processing step to encode the data in such a way that the puff-pastry effect is avoided. The encoding is not prefix-preserving and cannot be used in our CAS index. We need prefix searches to evaluate path predicates. The *c*-order and *z*-order curves are *static* interleaving schemes that do not take the data distribution into account. Indexes based on static schemes can be updated efficiently since insertions and deletions do not affect existing interleavings. The Variable UB-tree does not support incremental updates [24] since its encoding function adapts to the data distribution and must be recomputed whenever the data changes. Similarly, our data-driven dynamic interleaving does not support incremental updates since the position of the discriminative bytes may change when keys are inserted or deleted.

QUILTS [31] devises a static interleaving scheme for a specific query workload. Index updates, although not discussed, would work as for other static schemes (e.g., *c*- and *z*-order). Our dynamic interleaving adapts to the data distribution rather than a specific query workload. We do not optimize a specific workload but want to support a wide range of queries in a robust way, including ad-hoc queries.

4. BACKGROUND

Composite Keys. We use composite keys that consist of a path dimension P and value dimension V to index attributes in hierarchical data. Neither paths nor values nor the combination of paths and values need to be unique in a database. Composite keys can be extracted from popular semi-structured hierarchical data formats, such as JSON and XML.

Definition 1. (Composite Key) A composite key k states that a node with path $k.P$ in a database has value $k.V$.

Let $D \in \{P, V\}$ be the path or value dimension. We write $k.D$ to access k 's path (if $D = P$) or value (if $D = V$). The value dimension can be of any primitive data type. In the remainder of this paper we use one byte ASCII characters for the path dimension and hexadecimal numbers for the value dimension.

Example 2. In our running example we index attribute @weight. Table 1 shows the composite keys for the @weight attributes from the BOM in Figure 1. Since only the @weight attribute is indexed, we omit the label @weight in the paths in Table 1. The values of the @weight attribute are stored as 32 bit unsigned integers.

The set of composite keys in our running example is denoted by $K^{1..7} = \{k_1, k_2, \dots, k_7\}$, see Table 1. We use a sans-serif font to

Table 1: A set $K^{1..7} = \{k_1, \dots, k_7\}$ of composite keys. The values are stored as 32 bit unsigned integers.

	Path Dimension P	Value Dimension V
k_1	/bom/item/canoe\$	00 01 0E 50
k_2	/bom/item/carabiner\$	00 00 00 F1
k_3	/bom/item/car/battery\$	00 03 D3 5A
k_4	/bom/item/car/battery\$	00 03 D3 B0
k_5	/bom/item/car/belt\$	00 00 0B 4A
k_6	/bom/item/car/brake\$	00 00 0C C2
k_7	/bom/item/car/bumper\$	00 00 0A 8C
	1 3 5 7 9 11 13 15 17 19 21 23	1 2 3 4

refer to concrete values. Further, we use notation $K^{2,5,6,7}$ to refer to $\{k_2, k_5, k_6, k_7\}$.

Querying. Content-and-structure (CAS) queries contain a path predicate and value predicate [25]. The path predicate is expressed as a query path q that may include // to match a node itself and all its descendants, and the wildcard * to match all of a node's children. The latter is useful for data integrated from sources using different terminology (e.g., product instead of item in Fig. 1).

Definition 2. (Query Path) A query path q is denoted by $q = e_1 \lambda_1 e_2 \lambda_2 \dots \lambda_{m-1} e_m$. Each e_i , $i \leq m$, is either the path separator / or the descendant-or-self axis // that matches zero to any number of descendants. The final path separator e_m is optional. λ_i , $i < m$, is either a label or the wildcard * that matches any label.

Definition 3. (CAS Query) A CAS query $Q(q, \theta)$ consists of a query path q and a value predicate θ on an attribute A , where θ is a simple comparison $\theta = A \Theta v$ or a range comparison $\theta = v_l \Theta A \Theta' v_h$ where $\Theta, \Theta' \in \{=, <, >, \leq, \geq\}$. Let K be a set of composite keys. CAS query Q returns all composite keys $k \in K$ such that $k.P$ satisfies q and $k.V$ satisfies θ .

Example 3. The CAS query from Section 2 is expressed as $Q(/bom/item/car//, @weight \geq 50000)$ and returns all car parts weighing more than 50000 grams in Figure 1. CAS query $Q(/bom/*/car/battery, @capacity = 80000)$ looks for all car batteries that have a capacity of 80kWh. The wildcard * matches any child of bom (only item children exist in our example).

Representation of Keys. Paths and values are prefix-free byte strings as illustrated in Table 1. To get prefix-free byte strings we append the end-of-string character (ASCII code 0x00, here denoted by \$) to each path. This guarantees that no path is prefix of another path. Fixed-length byte strings (e.g., 32 bit numbers) are prefix-free because of the fixed length.

Let s be a byte-string, then $\text{len}(s)$ denotes the length of s and $s[i]$ denotes the i -th byte in s . The left-most byte of a byte-string is byte one. $s[i] = \epsilon$ is the empty string if $i > \text{len}(s)$. $s[i, j]$ denotes the substring of s from position i to j and $s[i, j] = \epsilon$ if $i > j$.

Interleaving of Composite Keys. We integrate path $k.P$ and value $k.V$ of a key k by interleaving them. Figure 2 shows various interleavings of key k_6 from Table 1. Value bytes are underlined and shown in red, path bytes are shown in blue. The first two rows show the two *c*-order curves: path-value and value-path concatenation (I_{PV} and I_{VP}). The byte-wise interleaving I_{BW} in the third row interleaves one value byte with one path byte. Note that none of these interleavings is well-balanced. The byte-wise interleaving is not well-balanced, since all value-bytes are interleaved

with parts of the common prefix of the paths (/bom/item/ca). In our experiments we use the surrogate-based extension proposed by Markl [24] to more evenly interleave dimensions of different lengths (see Section 7).

Approach	Interleaving of Key
$I_{PV}(k_6) = \text{/bom/item/car/brake\$ } \underline{00} \underline{00} \underline{0C} \underline{C2}$	
$I_{VP}(k_6) = \underline{00} \underline{00} \underline{0C} \underline{C2} \text{/bom/item/car/brake\$ }$	
$I_{BW}(k_6) = \underline{00} / \underline{00} \underline{b} \underline{0C} \underline{o} \underline{C2} \underline{m} / \text{item/car/brake\$ }$	

Figure 2: Key k_6 is interleaved using different approaches.

5. DYNAMIC INTERLEAVING

Our dynamic interleaving is a *data-driven* approach to interleave the paths and values of a set of composite keys K . It adapts to the specific characteristics of paths and values, such as varying length, differing domain sizes, and the skew of the data. To this end, we consider the distribution of *discriminative bytes* in the indexed data.

Definition 4. (Discriminative Byte) The discriminative byte of a set of composite keys K in dimension $D \in \{P, V\}$ is the position of the first byte in dimension D for which not all keys are equal:

$$\text{dsc}(K, D) = m \text{ iff}$$

$$\begin{aligned} & \exists k_i, k_j \in K, i \neq j (k_i.D[m] \neq k_j.D[m]) \text{ and} \\ & \forall k_i, k_j \in K, l < m (k_i.D[l] = k_j.D[l]) \end{aligned}$$

If all values of dimension D in K are equal, the discriminative byte does not exist. In this case we define $\text{dsc}(K, D) = \text{len}(k_i.D) + 1$ for some $k_i \in K$. \square

Example 4. Table 2 illustrates the position of the discriminative bytes for the path and value dimensions for various sets of composite keys K .

Table 2: Illustration of the discriminative bytes for $K^{1..7}$ from Table 1 and various subsets of it.

Composite Keys K	$\text{dsc}(K, P)$	$\text{dsc}(K, V)$
$K^{1..7}$	13	2
$K^{2,5,6,7}$	14	3
$K^{5,6,7}$	16	3
K^6	21	5

Discriminative bytes are crucial during query evaluation since at the position of the discriminative bytes the search space can be narrowed down. We alternate in a round-robin fashion between discriminative path and value bytes in our dynamic interleaving. Note that in order to determine the dynamic interleaving of a key k , which we denote by $I_{DY}(k, K)$, we have to consider the set of keys K to which k belongs and determine where the keys in K differ from each other (i.e., where their discriminative bytes are located). Each discriminative byte partitions K into subsets, which we recursively partition further.

5.1 Partitioning by Discriminative Bytes

The partitioning of a set of keys K groups composite keys together that have the same value for the discriminative byte in dimension D . Thus, K is split into at most 2^8 non-empty partitions, one partition for each value (0x00 to 0xFF) of the discriminative byte of dimension D .

Definition 5. (ψ -Partitioning) $\psi(K, D) = \{K_1, \dots, K_m\}$ is the ψ -partitioning of composite keys K in dimension D iff all partitions are non-empty ($K_i \neq \emptyset$ for $1 \leq i \leq m$), the number m of partitions is minimal, and:

1. All keys in partition $K_i \in \psi(K, D)$ have the same value for the discriminative byte of K in dimension D :

$$-\forall k_u, k_v \in K_i (k_u.D[\text{dsc}(K, D)] = k_v.D[\text{dsc}(K, D)])$$
2. The partitions are disjoint:

$$-\forall K_i, K_j \in \psi(K, D) (K_i \neq K_j \Rightarrow K_i \cap K_j = \emptyset)$$
3. The partitioning is complete:

$$-K = \bigcup_{K_i \in \psi(K, D)} K_i$$

Let $k \in K$ be a composite key. We write $\psi_k(K, D)$ to denote the ψ -partitioning of k with respect to K and dimension D , i.e., the partition in $\psi(K, D)$ that contains key k .

Example 5. Let $K^{1..7}$ be the set of composite keys from Table 1. The ψ -partitioning of selected sets of keys in dimension P or V is as follows:

- $\psi(K^{1..7}, V) = \{K^{2,5,6,7}, K^1, K^{3,4}\}$
- $\psi(K^{2,5,6,7}, P) = \{K^2, K^{5,6,7}\}$
- $\psi(K^{5,6,7}, V) = \{K^5, K^6, K^7\}$
- $\psi(K^6, V) = \psi(K^6, P) = \{K^6\}$

The ψ -partitioning of key k_6 with respect to sets of keys and dimensions is as follows:

- $\psi_{k_6}(K^{1..7}, V) = K^{2,5,6,7}$
- $\psi_{k_6}(K^6, V) = \psi_{k_6}(K^6, P) = K^6$

The crucial property of our partitioning is that the position of the discriminative byte for dimension D increases if we ψ -partition K in D . This *monotonicity* property of the ψ -partitioning holds since every partition is built based on the discriminative byte and to partition an existing partition we need a discriminative byte that will be positioned further down in the byte-string. For the alternate dimension \bar{D} , i.e., $\bar{D} = P$ if $D = V$ and $\bar{D} = V$ if $D = P$, the position of the discriminative byte remains unchanged or may increase.

LEMMA 1. (Monotonicity of Discriminative Bytes) Let $K_i \in \psi(K, D)$ be one of the partitions of K after partitioning in dimension D . In dimension D , the position of the discriminative byte in K_i is strictly greater than in K while, in dimension \bar{D} , the discriminative byte is equal or greater than in K , i.e.,

$$K_i \in \psi(K, D) \wedge K_i \subset K \Rightarrow$$

$$\text{dsc}(K_i, D) > \text{dsc}(K, D) \wedge \text{dsc}(K_i, \bar{D}) \geq \text{dsc}(K, \bar{D})$$

We provide the proofs for all lemmas and theorems in a technical report [40].

Example 6. The discriminative path byte of $K^{1..7}$ is 13 while the discriminative value byte of $K^{1..7}$ is 2 as shown in Table 2. For partition $K^{2,5,6,7}$, which is obtained by partitioning $K^{1..7}$ in the value dimension, the discriminative path byte is 14 while the discriminative value byte is 3. The positions of both discriminative bytes have increased. For partition $K^{5,6,7}$, which is obtained by partitioning $K^{2,5,6,7}$ in the path dimension, the discriminative path byte is 16 while the discriminative value byte is 3. The position of the discriminative path byte has increased while the position of the discriminative value byte has not changed.

When computing the dynamic interleaving of a composite key $k \in K$ we recursively ψ -partition K while alternating between dimension V and P . This yields a partitioning sequence $(K_1, D_1), \dots, (K_n, D_n)$ for key k with $K_1 \supseteq K_2 \supseteq \dots \supseteq K_n$. We start with $K_1 = K$ and $D_1 = V$. Next, $K_2 = \psi_k(K_1, V)$ and $D_2 = \overline{D_1} = P$. We continue with the general scheme $K_{i+1} = \psi_k(K_i, D_i)$ and $D_{i+1} = \overline{D_i}$. This goes on until we run out of discriminative bytes in one dimension, which means $\psi_k(K, D) = K$. From then on, we can only partition in dimension \overline{D} . When we run out of discriminative bytes in this dimension as well, that is $\psi_k(K, \overline{D}) = \psi_k(K, D) = K$, we stop. The partitioning sequence is finite due to the monotonicity of the ψ -partitioning (see Lemma 1), which guarantees that we make progress in every step in at least one dimension. Below we define a partitioning sequence.

Definition 6. (Partitioning Sequence) The partitioning sequence $\rho(k, K, D) = ((K_1, D_1), \dots, (K_n, D_n))$ of a composite key $k \in K$ denotes the recursive ψ -partitioning of the partitions to which k belongs. The pair (K_i, D_i) denotes the partitioning of K_i in dimension D_i . The final partition K_n cannot be partitioned further, hence $D_n = \perp$. $\rho(k, K, D)$ is defined as follows:¹

$$\rho(k, K, D) = \begin{cases} (K, D) \circ \rho(k, \psi_k(K, D), \overline{D}) & \text{if } \psi_k(K, D) \subset K \\ \rho(k, K, \overline{D}) & \text{if } \psi_k(K, D) = K \wedge \psi_k(K, \overline{D}) \subset K \\ (K, \perp) & \text{otherwise} \end{cases}$$

Example 7. In the following we illustrate the step-by-step expansion of $\rho(k_6, K^{1..7}, V)$ to get k_6 's partitioning sequence.

$$\begin{aligned} \rho(k_6, K^{1..7}, V) &= \\ &= (K^{1..7}, V) \circ \rho(k_6, K^{2..5,6,7}, P) \\ &= (K^{1..7}, V) \circ (K^{2..5,6,7}, P) \circ \rho(k_6, K^{5,6,7}, V) \\ &= (K^{1..7}, V) \circ (K^{2..5,6,7}, P) \circ (K^{5,6,7}, V) \circ \rho(k_6, K^6, P) \\ &= (K^{1..7}, V) \circ (K^{2..5,6,7}, P) \circ (K^{5,6,7}, V) \circ (K^6, \perp) \end{aligned}$$

Notice the alternating partitioning in, respectively, V and P . We only deviate from this if partitioning in one of the dimensions is not possible. For instance, $K^{3..4}$ cannot be partitioned in dimension P and therefore we get

$$\rho(k_4, K^{1..7}, V) = (K^{1..7}, V) \circ (K^{3..4}, V) \circ (K^4, \perp) \quad \square$$

There are two key ingredients to our dynamic interleaving: the monotonicity of discriminative bytes (Lemma 1) and the alternating ψ -partitioning (Definition 6). The monotonicity guarantees that each time we ψ -partition K we advance the discriminative byte in at least one dimension. The alternating ψ -partitioning ensures that we interleave paths and values.

5.2 Interleaving

We determine the dynamic interleaving $I_{DY}(k, K)$ of a key $k \in K$ via k 's partitioning sequence ρ . For each element in ρ , we generate a tuple containing two strings s_P and s_V and the partitioning dimension of the element. The strings s_P and s_V are composed of substrings of $k.P$ and $k.V$, ranging from the previous discriminative byte up to, but excluding, the current discriminative byte in the respective dimension. The order of s_P and s_V in a tuple depends on the dimension used in the previous step: the dimension that has been chosen for the partitioning comes first. Formally, this is defined as follows:

¹Operator \circ denotes concatenation, e.g., $a \circ b = (a, b)$ and $a \circ (b, c) = (a, b, c)$

Definition 7. (Dynamic Interleaving) Let $k \in K$ be a composite key and let $\rho(k, K, V) = ((K_1, D_1), \dots, (K_n, D_n))$ be the partitioning sequence of k . The dynamic interleaving $I_{DY}(k, K) = (t_1, \dots, t_n)$ of k is a sequence of tuples t_i , where $t_i = (s_P, s_V, D)$ if $D_{i-1} = P$ and $t_i = (s_V, s_P, D)$ if $D_{i-1} = V$. The path and value substrings, s_P and s_V , and the partitioning dimension D are determined as follows:

$$\begin{aligned} t_i.s_P &= k.P[\text{dsc}(K_{i-1}, P), \text{dsc}(K_i, P) - 1] \\ t_i.s_V &= k.V[\text{dsc}(K_{i-1}, V), \text{dsc}(K_i, V) - 1] \\ t_i.D &= D_i \end{aligned}$$

To correctly handle the first tuple we define $\text{dsc}(K_0, V) = 1$, $\text{dsc}(K_0, P) = 1$ and $D_0 = V$. \square

Example 8. We compute the tuples for the dynamic interleaving $I_{DY}(k_6, K^{1..7}) = (t_1, \dots, t_4)$ of key k_6 using the partitioning sequence $\rho(k_6, K^{1..7}, V) = ((K^{1..7}, V), (K^{2..5,6,7}, P), (K^{5,6,7}, V), (K^6, \perp))$ from Example 7. The necessary discriminative path and value bytes can be found in Table 2. Table 3 shows the details of each tuple of k_6 's dynamic interleaving with respect to $K^{1..7}$.

Table 3: Computing the dynamic interleaving $I_{DY}(k_6, K^{1..7})$.

t	s_V	s_P	D
t_1	$k_6.V[1, 1] = \underline{\text{00}}$	$k_6.P[1, 12] = \underline{/bom/item/ca}$	V
t_2	$k_6.V[2, 2] = \underline{\text{00}}$	$k_6.P[13, 13] = \underline{r}$	P
t_3	$k_6.V[3, 2] = \underline{\epsilon}$	$k_6.P[14, 15] = \underline{/b}$	V
t_4	$k_6.V[3, 4] = \underline{0C}\ \underline{C2}$	$k_6.P[16, 20] = \underline{rake\$}$	\perp

The final dynamic interleavings of all keys from Table 1 are displayed in Table 4. We highlight in bold the values of the discriminative bytes at which the paths and values are interleaved, e.g., for key k_6 these are bytes $\underline{\text{00}}$, $\underline{/}$, and $\underline{0C}$.

Table 4: The dynamic interleaving of the composite keys in $K^{1..7}$. The values of the discriminative bytes are written in bold.

k	Dynamic Interleaving $I_{DY}(k, K^{1..7})$
k_2	$((\underline{\text{00}}, \underline{/b} \dots a, V), (\underline{\text{00}}, \underline{r}, P), (\underline{\text{abiner\$}}, \underline{\text{00 F1}}, \perp))$
k_7	$((\underline{\text{00}}, \underline{/b} \dots a, V), (\underline{\text{00}}, \underline{r}, P), (\underline{/b}, \underline{\epsilon}, V), (\underline{\text{0A 8C}}, \underline{\text{umper\$}}, \perp))$
k_5	$((\underline{\text{00}}, \underline{/b} \dots a, V), (\underline{\text{00}}, \underline{r}, P), (\underline{/b}, \underline{\epsilon}, V), (\underline{\text{0B 4A}}, \underline{\text{elt\$}}, \perp))$
k_6	$((\underline{\text{00}}, \underline{/b} \dots a, V), (\underline{\text{00}}, \underline{r}, P), (\underline{/b}, \underline{\epsilon}, V), (\underline{\text{OC C2}}, \underline{\text{rake\$}}, \perp))$
k_1	$((\underline{\text{00}}, \underline{/b} \dots a, V), (\underline{\text{01 0E 50}}, \underline{\text{noe\$}}, \perp))$
k_3	$((\underline{\text{00}}, \underline{/b} \dots a, V), (\underline{\text{03 D3}}, \underline{\text{r/battery\$}}, V), (\underline{\text{5A}}, \underline{\epsilon}, \perp))$
k_4	$((\underline{\text{00}}, \underline{/b} \dots a, V), (\underline{\text{03 D3}}, \underline{\text{r/battery\$}}, V), (\underline{\text{B0}}, \underline{\epsilon}, \perp))$

5.3 Efficiency of Interleavings

We introduce a cost model to measure the efficiency of different interleaving schemes. We assume that the interleaved keys are arranged in a tree-like search structure. Each node represents the partitioning of the composite keys by either path or value, and the node branches for each different value of a discriminative path or value byte. We simplify the cost model by assuming that the search structure is a complete tree with fanout o where every root-to-leaf path contains h edges (h is called the height). Further, we assume that all nodes on one level represent a partitioning in the same dimension ϕ_i and we use a vector $\phi(\phi_1, \dots, \phi_h)$ to specify the partitioning dimension on each level. Figure 3 visualizes this scheme.

A search starts at the root and traverses the data structure to determine the answer set. In the case of range queries, more than one branch must be followed. A search follows a fraction of the outgoing branches o originating at this node. We call this the selectivity of a node (or just selectivity). We assume that every path node has a selectivity of s_P and every value node has the selectivity of s_V .

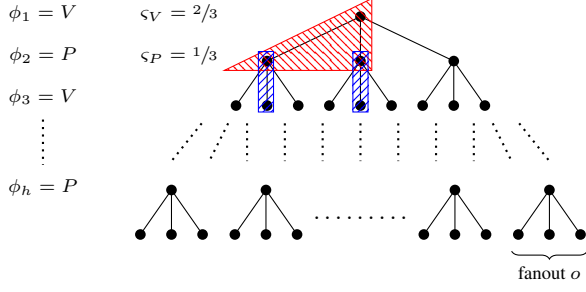


Figure 3: The search structure in our cost model is a complete tree of height h and fanout o .

The cost \hat{C} of a search, measured in the number of visited nodes during the search, is as follows:

$$\hat{C}(o, h, \phi, \varsigma_P, \varsigma_V) = 1 + \sum_{l=1}^h \prod_{i=1}^l (o \cdot \varsigma_{\phi_i})$$

If a workload is known upfront, a system can optimize indexes to support specific queries. Our goal is an access method that can deal with a wide range of queries in a dynamic environment in a robust way, i.e., avoiding a bad performance for any particular query type. This is motivated by the fact that modern data analytics utilizes a large number of ad-hoc queries to do exploratory analysis. For example, in the context of building a robust partitioning scheme for ad-hoc query workloads, Shanbhag et al. [38] found that after analyzing the first 80% of real-world workload traces the remaining 20% still contained 57% completely new queries.

Even though robustness of query processing performance has received considerable interest, there is a lack of unified metrics in this area [16, 17]. Our goal is a good performance for queries with differing selectivities for path and value predicates. Towards this goal we define the notion of *complementary queries*.

Definition 8. (Complementary Query) Given a query Q with path selectivity ς_P and value selectivity ς_V , there is a *complementary query* Q' with path selectivity $\varsigma'_P = \varsigma_V$ and value selectivity $\varsigma'_V = \varsigma_P$

State-of-the-art CAS-indexes favor either path or value predicates. As a result they show a very good performance for one type of query but run into problems for the complementary query.

Definition 9. (Robustness) A CAS-index is *robust* if it optimizes the average performance when evaluating a query Q and its complementary query Q' .

Example 9. Figure 4a shows the costs for a query Q and its complementary query Q' for different interleavings in terms of the number of visited nodes during the search. We assume parameters $o = 10$ and $h = 12$ for the search structure. In our dynamic interleaving I_{DY} the discriminative bytes are perfectly alternating. I_{PV} stands for path-value concatenation with $\phi_i = P$ for $1 \leq i \leq 6$ and $\phi_i = V$ for $7 \leq i \leq 12$. I_{VP} is a value-path concatenation (with an inverse ϕ compared to I_{PV}). We also consider two additional permutations: I_1 uses a vector $\phi = (V, V, V, V, P, V, P, V, P, P, P)$ and I_2 one equal to $(V, V, V, P, P, V, P, V, V, P, P, P)$. They resemble, e.g., the byte-wise interleaving that usually exhibits irregular alternation patterns with a clustering of, respectively, discriminative path and value bytes. Figure 4b shows the average costs and the standard deviation. The numbers demonstrate the robustness of our dynamic

interleaving: it clearly shows the best performance both in terms of average costs and lowest standard deviation.

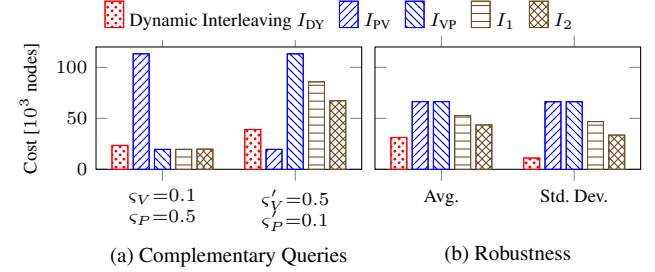


Figure 4: Dynamic interleaving has a robust query performance.

In the previous example we showed empirically that a perfectly alternating interleaving exhibits the best overall performance when evaluating complementary queries. In addition to this, we can prove that this is always the case.

THEOREM 2. Consider a query Q with selectivities ς_P and ς_V and its complementary query Q' with selectivities $\varsigma'_P = \varsigma_V$ and $\varsigma'_V = \varsigma_P$. There is no interleaving that on average performs better than the dynamic interleaving that has a perfectly alternating vector ϕ_{DY} , i.e., $\forall \phi : \hat{C}(o, h, \phi_{DY}, \varsigma_P, \varsigma_V) + \hat{C}(o, h, \phi_{DY}, \varsigma'_P, \varsigma'_V) \leq \hat{C}(o, h, \phi, \varsigma_P, \varsigma_V) + \hat{C}(o, h, \phi, \varsigma'_P, \varsigma'_V)$.

See [40] for the proof. Note that in practice the search structure is not a complete tree and the fraction ς_P and ς_V of children that are traversed at each node is not constant. In Section 7.4 we experimentally evaluate the cost model on real-world datasets. We show that the estimated cost and the true cost of a query are off by a factor of two, on average. This is a good estimate for the cost of a query.

6. RCAS INDEX

We propose the Robust Content-And-Structure (RCAS) index to efficiently query the content and structure of hierarchical data. The RCAS index uses our dynamic interleaving to integrate the paths and values of composite keys in a trie-based index.

6.1 Trie-Based Structure of RCAS

The RCAS index is a trie data-structure that efficiently supports CAS queries with range and prefix searches. Each node n in the RCAS index includes a dimension $n.D$, path substring $n.s_P$, and value substring $n.s_V$ that correspond to the fields $t.D$, $t.s_P$ and $t.s_V$ in the dynamic interleaving of a key (see Definition 7). The substrings $n.s_P$ and $n.s_V$ are variable-length strings. Dimension $n.D$ is P or V for inner nodes and \perp for leaf nodes. Leaf nodes additionally store a set of references r_i to nodes in the database, denoted $n.refs$. Each dynamically interleaved key corresponds to a root-to-leaf path in the RCAS index.

Definition 10. (RCAS Index) Let K be a set of composite keys and let R be a tree. Tree R is the RCAS index for K iff the following conditions are satisfied.

1. $I_{DY}(k, K) = (t_1, \dots, t_m)$ is the dynamic interleaving of a key $k \in K$ iff there is a root-to-leaf path (n_1, \dots, n_m) in R such that $t_i.s_P = n_i.s_P$, $t_i.s_V = n_i.s_V$, and $t_i.D = n_i.D$ for $1 \leq i \leq m$.

2. R does not include duplicate siblings, i.e., no two sibling nodes n and n' , $n \neq n'$, in R have the same values for s_P , s_V , and D , respectively.

Example 10. Figure 5 shows the RCAS index for the composite keys $K^{1..7}$. We use blue and red colors for bytes from the path and value, respectively. The discriminative bytes are highlighted in bold. The dynamic interleaving $I_{DY}(k_6, K^{1..7}) = (t_1, t_2, t_3, t_4)$ from Table 4 is mapped to the path (n_1, n_2, n_4, n_7) in the RCAS index. For key k_2 , the first two tuples of $I_{DY}(k_2, K^{1..7})$ are also mapped to n_1 and n_2 , while the third tuple is mapped to n_3 .

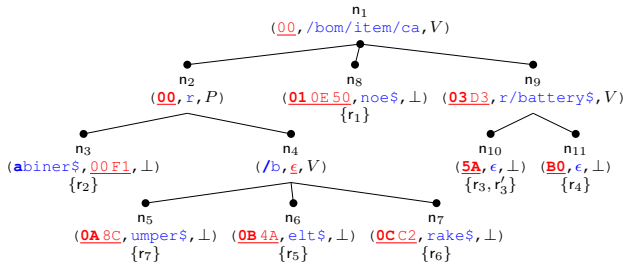


Figure 5: The RCAS index for the composite keys $K^{1..7}$.

6.2 Physical Node Layout

Figure 6 shows the physical structure of an inner node. The header field contains meta information, such as the number of children. Fields s_P and s_V (explained above) are implemented as variable-length byte vectors ($C++\text{std}::vector<\text{uint8_t}>$). Dimension D (P or V , or \perp if the node is a leaf) is the dimension in which the node partitions the data. The remaining space of an inner node (gray-colored in Figure 6) is reserved for child pointers. Since ψ partitions at the granularity of bytes, each node can have at most 256 children, one for each possible value of a discriminative byte from 0x00 to 0xFF (or their corresponding ASCII characters in Figure 5). For each possible value b there is a pointer to the subtree whose keys all have value b for the discriminative byte of dimension D . Typically, many of the 256 pointers are NULL. Therefore, we implement our trie as an Adaptive Radix Tree (ART) [21], which defines four node types with a physical fanout of 4, 16, 48, and 256 child pointers, respectively. Nodes are resized to adapt to the actual fanout of a node. Figure 6 illustrates the node type with an array of 256 child pointers. For the remaining node types we refer to Leis et al. [21].

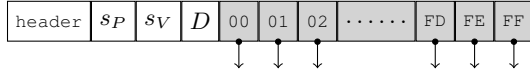


Figure 6: Structure of an inner node with 256 pointers.

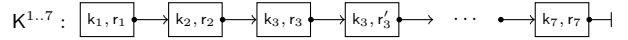
The structure of a leaf node is similar to that shown in Figure 6, except that instead of child pointers the leaf nodes have a variable-length vector with references to nodes in the database.

6.3 Bulk-Loading RCAS

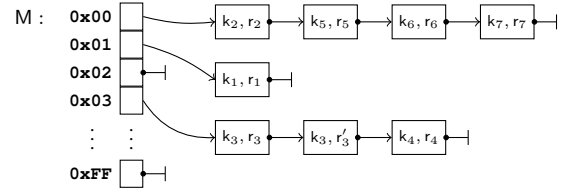
This section gives an efficient bulk-loading algorithm for RCAS that is linear in the number of composite keys $|K|$. It simultaneously computes the dynamic interleaving of all keys in K . We implement a partition K as a linked list of pairs (k, r) , where r is a

reference to a database node with path $k.P$ and value $k.V$. In our implementation the keys in K need not be unique. There can be pairs (k, r_i) and (k, r_j) that have the same key but have different references $r_i \neq r_j$. This is the case if there are different nodes in the indexed database that have the same path and value (thus the same key). A partitioning $M = \psi(K, D)$ is implemented as an array of length 2^8 with references to (possibly empty) partitions K . The array indexes 0x00 to 0xFF are the values of the discriminative byte.

Example 11. Figure 7a shows the linked list for set $K^{1..7}$ from our running example. Two nodes, pointed to by r_3 and r'_3 , have the same key k_3 . They correspond to the batteries in Figure 1 that have the same path and value. Figure 7b shows the partitioning $\psi(K^{1..7}, V)$ for our running example. Three partitions exist with values **0x00**, **0x01**, and **0x03** for the discriminative value byte.



(a) Partition $K^{1..7}$ is represented as a list of (k, r) pairs.



(b) The partitioning $M = \psi(K^{1..7}, V)$ is an array with 2^8 partitions.

Figure 7: Data structures used in Algorithm 3.

Algorithm 1 determines the discriminative byte for a partition K . Note that $dsc.inc$ looks for the discriminative byte starting from position g , where g is a lower bound for $dsc(K, D)$ as per Lemma 1. Also, looping through the bytes of the first key of K is correct even if there are shorter keys in K . Since we use prefix-free keys, any shorter keys differ at some position, terminating the loop correctly.

Algorithm 1: $dsc.inc(K, D, g)$

```

1 Let  $(k_i, r_i)$  be the first key in  $K$ ;
2 while  $g \leq \text{len}(k_i.D)$  do
3   for  $(k_j, r_j) \in K$  do
4     if  $k_j.D[g] \neq k_i.D[g]$  then return  $g$ ;
5    $g++$ ;
6 return  $g$ 

```

Algorithm 2 illustrates the computation of the ψ -partitioning $M = \psi(K, D, g)$. We pass the position g of the discriminative byte for dimension D as an argument to ψ . The discriminative byte determines the partition to which a key belongs.

Algorithm 2: $\psi(K, D, g)$

```

1 Let  $M$  be an array of  $2^8$  empty lists;
2 for  $(k_i, r_i) \in K$  do
3   Move  $(k_i, r_i)$  from partition  $K$  to partition  $M[k_i.D[g]]$ ;
4 return  $M$ 

```

Algorithm 3 recursively ψ -partitions K and alternates between the path and value dimensions. In each call of BulkLoadRCAS one

new node n is added to the index. The algorithm takes four parameters: (a) partition K , (b) dimension $D \in \{P, V\}$ by which K is partitioned, and the positions of the previous discriminative (c) path byte g_P and (d) value byte g_V . For the first call, when no previous discriminative path and value bytes exist, we set $g_P = g_V = 1$. BulkLoadRCAS($K, V, 1, 1$) returns a pointer to the root node of the new RCAS index. We start by creating a new node n (line 1) and determining the discriminative path and value bytes g'_P and g'_V of K (lines 3-4). Lemma 1 guarantees that the previous discriminative bytes g_P and g_V are valid lower bounds for g'_P and g'_V , respectively. Next, we determine the current node's substrings s_P and s_V in lines 5-6 (see Definition 7). In lines 7-10 we check for the base case of the recursion, which occurs when all discriminative bytes are exhausted and K cannot be partitioned further. In this case, all remaining pairs $(k, r) \in K$ have the same key k . Leaf node n contains the references to nodes in the database with this particular key k . In lines 11 we check if K can be partitioned in dimension D . If this is not the case, since all keys have the same value in dimension D , we ψ -partition K in the alternate dimension \bar{D} . Finally, in lines 14-16 we iterate over all non-empty partitions in M and recursively call the algorithm for each partition $M[b]$, alternating dimension D in round-robin fashion.

Algorithm 3: BulkLoadRCAS(K, D, g_P, g_V)

```

1 Let  $n$  be a new RCAS node;
2 Let  $(k_i, r_i)$  be the first key in  $K$ ;
3  $g'_P \leftarrow \text{dsc.inc}(K, P, g_P)$ ;
4  $g'_V \leftarrow \text{dsc.inc}(K, V, g_V)$ ;
5  $n.s_P \leftarrow k_i.P[g_P, g'_P - 1]$ ;
6  $n.s_V \leftarrow k_i.V[g_V, g'_V - 1]$ ;
7 if  $g'_P > \text{len}(k_i.P) \wedge g'_V > \text{len}(k_i.V)$  then /*  $n$  is a leaf */
8    $n.D \leftarrow \perp$ ;
9   for  $(k_j, r_j) \in K$  do append  $r_j$  to  $n.\text{refs}$ ;
10  return  $n$ ;
11 if  $g'_D > \text{len}(k_i.D)$  then  $D \leftarrow \bar{D}$ ;
12  $n.D \leftarrow D$ ;
13  $M \leftarrow \psi(K, D, g'_D)$ ;
14 for  $b \leftarrow 0x00$  to  $0xFF$  do
15   if partition  $M[b]$  is not empty then
16      $n.\text{children}[b] \leftarrow \text{BulkLoadRCAS}(M[b], \bar{D}, g'_P, g'_V)$ ;
17 return  $n$ 

```

LEMMA 3. Let K be a set of composite keys and let $l = \max_{k \in K} \{\text{len}(k.P) + \text{len}(k.V)\}$ be the length of the longest key. The time complexity of Algorithm 3 is $O(l \cdot |K|)$.

See [40] for the proof. The factor l in the complexity of Algorithm 3 is typically much smaller than $\text{len}(k.P) + \text{len}(k.V)$ of the longest key k . For instance, assuming a combined length of just six bytes would already give us around 280 trillion potentially different keys. So, we would need a huge number of keys for every byte to become a discriminative byte on each recursion level.

6.4 Querying RCAS

Algorithm 4 shows the pseudocode for evaluating a CAS query on an RCAS index. The function CasQuery gets called with the current node n (initially the root node of the index), a path predicate consisting of a query path q , and a range $[v_l, v_h]$ for the value predicate. Furthermore, we need two buffers buff_P and buff_V (initially empty) that hold, respectively, all path and value bytes

from the root to the current node n . Finally, we require state information s to evaluate the path and value predicates (we provide details as we go along) and an answer set W to collect the results.²

Algorithm 4: CasQuery($n, q, [v_l, v_h], \text{buff}_V, \text{buff}_P, s, W$)

```

1  $\text{UpdateBuffers}(n, \text{buff}_V, \text{buff}_P)$ 
2  $\text{match}_V \leftarrow \text{MatchValue}(\text{buff}_V, v_l, v_h, s, n)$ 
3  $\text{match}_P \leftarrow \text{MatchPath}(\text{buff}_P, q, s, n)$ 
4 if  $\text{match}_V = \text{MATCH}$  and  $\text{match}_P = \text{MATCH}$  then
5   | Collect( $n, W$ )
6 else if  $\text{match}_V \neq \text{MISMATCH}$  and  $\text{match}_P \neq \text{MISMATCH}$  then
7   | for each matching child  $c$  in  $n$  do
8     |   |  $s' \leftarrow \text{Update}(s)$ 
9     |   | CasQuery( $c, q, [v_l, v_h], \text{buff}_V, \text{buff}_P, s', W$ )

```

First, we update the buffers buff_V and buff_P , adding the information in the fields s_V and s_P of the current node n (line 1). Next, we match the query predicates to the current node. Matching values (line 2) works differently to matching paths (line 3), so we look at the two cases separately.

To match the current (partial) value buff_V against the value range $[v_l, v_h]$, their byte strings must be binary comparable (for a detailed definition of binary-comparability see [21]). Function MatchValue proceeds as follows. We compute the longest common prefix between buff_V and v_l and between buff_V and v_h . We denote the position of the first byte for which buff_V and v_l differ by lo and the position of the first byte for which buff_V and v_h differ by hi . If $\text{buff}_V[\text{lo}] < v_l[\text{lo}]$, we know that the node's value lies outside of the range and we return MISMATCH. Similarly, if $\text{buff}_V[\text{hi}] > v_h[\text{hi}]$, the node's value lies outside of the upper bound and we return MISMATCH as well. If n is a leaf node and $v_l \leq \text{buff}_V \leq v_h$, we return MATCH. If n is not a leaf node and $v_l[\text{lo}] < \text{buff}_V[\text{lo}]$ and $\text{buff}_V[\text{hi}] < v_h[\text{hi}]$, we know that all values in the subtree rooted at n match and we also return MATCH. In all other cases we cannot make a decision yet and return INCOMPLETE. The values of lo and hi are kept in the state to avoid recomputing the longest common prefix from scratch for each node. Instead we can resume the search from the previous values of lo and hi .

Function MatchPath matches the query path q against the current path prefix buff_P . It supports the wildcard symbol $*$ and the descendant-or-self axis $//$ that match any child and descendant node, respectively. As long as we do not encounter any wildcards in the query path q , we directly compare (a prefix of) q with the current content of buff_P byte by byte. As soon as a byte does not match, we return MISMATCH. If we are able to successfully match the complete query path q against a complete path in buff_P (both terminated by $\$$), we return MATCH. Otherwise, we need to continue and return INCOMPLETE. When we encounter a wildcard $*$ in q , we match it successfully to the corresponding label in buff_P and continue with the next label. A wildcard $*$ itself will not cause a mismatch (unless we try to match it against the terminator $\$$), so we either return MATCH if it is the final label in q and buff_P or INCOMPLETE. Matching the descendant-axis $//$ is more complicated. We note the current position where we are in buff_P and continue matching the label after $//$ in q . If at any point we find a mismatch, we backtrack to the next path separator after the noted position, thus skipping a label in buff_P and restarting the search from there. Once buff_P contains a complete path, we can make a decision between MATCH or MISMATCH.

²The parameters n , W , q , and $[v_l, v_h]$ are call-by-reference, the parameters buff_V , buff_P , and s are call-by-value.

The algorithm continues by checking the outcomes of the value and path matching (lines 4 and 6). If both predicates match, we descend the subtree and collect all references (line 5 and function `Collect` in Algorithm 5). If at least one of the outcomes is `MISMATCH`, we immediately stop the search in the current node, otherwise we continue recursively with the matching children of n (lines 7–9). Finding the matching children depends on the dimension $n.D$ of n and follows the same logic as described above for `MatchValue` and `MatchPath`. If node $n.D = P$ and we have seen a descendant axis in the query path, all children of the current node match.

Algorithm 5: `Collect(n, W)`

```

1 if  $n$  is a leaf then
2   | add references  $r$  in  $n.\text{refs}$  to  $W$ 
3 else
4   | for each child  $c$  in  $n$  do
5     |   | Collect( $c, W$ )

```

Example 12. We consider an example CAS query with path $q = \text{/bom/item//battery\$}$ and a value range from $v_l = 10^5 = \text{00 01 86 A0}$ to $v_h = 5 \cdot 10^5 = \text{00 07 A1 20}$. We execute the query on the index depicted in Figure 5.

- Starting at the root node n_1 , we load `00` and `/bom/item/ca` into buff_V and buff_P , respectively. Function `MatchValue` matches `00` and returns `INCOMPLETE`. `MatchPath` also returns `INCOMPLETE`: even though it matches `/bom/item`, the partial label `ca` does not match `battery`, so `ca` is skipped by the descendant axis. Since both functions return `INCOMPLETE`, we have to traverse all matching children. Since n_1 is a value node ($n_1.D = V$), we look for all matching children whose discriminative value byte is between `01` and `07`. Nodes n_8 and n_9 satisfy this condition.
- Node n_8 is a leaf. buff_P and buff_V are updated and contain complete paths and values. Byte `01` matches, but byte $\text{buff}_V[3] = \text{0E} < \text{86} = v_l[3]$. Thus, `MatchValue` returns a `MISMATCH`. So does `MatchPath`. The search discards n_8 .
- Next we look at node n_9 . We find that $v_l[2] < \text{buff}_V[2] < v_h[2]$, thus all values of n_9 's descendants are within the bounds v_l and v_h , and `MatchValue` returns `MATCH`. `MatchPath` skips the next bytes `r/` due to the descendant axis and resumes matching from there. After skipping `r/`, it returns `MATCH`, as `battery$` matches the query path until its end. Both predicates match, invoking `Collect` on n_9 , which traverses n_9 's descendants n_{10} and n_{11} and adds references r_3, r'_3 , and r_4 to W .

Twig queries [4] with predicates on multiple attributes are broken into smaller CAS queries. Each root-to-leaf branch of the twig query is evaluated independently on an appropriate RCAS index and the resulting sets W are joined to produce the final result. The join requires that the references $r \in W$ contain structural information about a node's position in the tree (e.g., an `OrdPath` [32] node-labeling scheme). A query optimizer can use our cost model to choose which RCAS indexes are used in a query plan.

7. EXPERIMENTAL EVALUATION

7.1 Setup and Datasets

We use a virtual Ubuntu 18.04 server with eight cores and 64GB of main memory. All algorithms are implemented in C++ by the same author and were compiled with clang 6.0.0 using `-O3`. Each

Table 5: Dataset Statistics

Dataset	Size	Attribute	No. of Keys	Unique Keys	Size of Keys
ServerFarm	3.0GB	size	21'291'019	9'345'668	1.7GB
XMark	58.9GB	category	60'272'422	1'506'408	3.3GB
Amazon	10.5GB	price	6'707'397	6'461'587	0.8GB

reported runtime measurement is the average of 100 runs. All indexes are kept in main memory. The code³ and the datasets⁴ used in the experimental evaluation can be found online.

Datasets. We use three datasets, the ServerFarm dataset that we collected ourselves, a product catalog with products from Amazon [18], and the synthetic XMark [37] dataset at a scale factor of 500. The ServerFarm dataset mirrors the file system of 100 Linux servers. For each server we installed a default set of packages and randomly picked a subset of optional packages. In total there are 21 million files. For each file we record the file's full path, size, various timestamps (e.g., a file's change time `ctime`), file type, extension etc. The Amazon dataset [18] contains products that are hierarchically categorized. For each experiment we index the paths in a dataset along with one of its attributes. We use the notation `$dataset:$attribute` to indicate which attribute in a dataset is indexed. E.g., `ServerFarm:size` contains the path of each file in the ServerFarm dataset along with its size. The datasets do not have to fit into main memory, but we assume that the indexed keys fit into main memory. Table 5 shows a summary of the datasets.

Compared Approaches. We compare our RCAS index based on dynamic interleaving with the following approaches that can deal with variable-length keys. The path-value (PV) and value-path (VP) concatenations are the two possible c -order curves [31]. The next approach, termed ZO for z -order [29, 33], maps variable-length keys to a fixed length as proposed by Markl [24]. Each path label is mapped to a fixed length using a surrogate function. Since paths can have a different number of labels, shorter paths are padded with empty labels to match the number of labels in the longest path in the dataset. The resulting paths have a fixed length l_P and are interleaved with values of length l_V such that $\lceil l_V/l_P \rceil$ value bytes are followed by $\lceil l_P/l_V \rceil$ path bytes. The label-wise interleaving (LW) interleaves one byte of the value with one label of the path. We utilize our RCAS index to identify the dimension of every byte of the variable-length interleaved keys. The same underlying data-structure is also used to store the keys generated by PV, VP, and ZO. Finally, we compare RCAS against the CAS index in [25] that builds a structural summary (DataGuide [15]) and a value index (B+ tree⁵) and joins them to answer CAS queries. We term this approach XML as it was proposed for XML databases.

7.2 Impact of Datasets on RCAS's Structure

In Figure 8 we show how the shape (depth and width) of the RCAS index adapts to the datasets. Figure 8a shows the distribution of the node depths in the RCAS index for the `ServerFarm:size` dataset. Because of the trie-based structure not every root-to-leaf path in RCAS has the same length (see also Figure 5). The deepest nodes occur on level 33, but most nodes occur on levels 10 to 15 with an average node depth of 13.2. This is due to the different lengths of the paths in a file system. Figure 8b shows the number of nodes for each node type. Recall from Section 6.2 that RCAS, like ART [21], uses inner nodes with a physical fanout of 4, 16, 48, and 256 pointers depending on the actual fanout of a node to reduce the

³<https://github.com/k13n/rcas>

⁴<https://doi.org/10.5281/zenodo.3739263>

⁵We use the tlx B+ tree (<https://github.com/tlx/tlx>), used also by [6, 41] for comparisons.

Table 6: CAS queries with their result size and the number of keys that match the path, respectively value predicate.

Query Q	Result size (σ)	Matching paths (σ_P)	Matching values (σ_V)
Dataset: ServerFarm:size			
Q_1 $Q(/usr/include//, @size \geq 5000)$	142253 (0.6%)	434564 (2.0%)	7015066 (32.9%)
Q_2 $Q(/usr/include//, 3000 \leq @size \leq 4000)$	46471 (0.2%)	434564 (2.0%)	1086141 (5.0%)
Q_3 $Q(/usr/lib//, 0 \leq @size \leq 1000)$	512497 (2.4%)	2277518 (10.6%)	8403809 (39.4%)
Q_4 $Q(/usr/share//Makefile, 1000 \leq @size \leq 2000)$	1193 (< 0.1%)	6408 (< 0.1%)	2494804 (11.7%)
Q_5 $Q(/usr/share/doc//README, 4000 \leq @size \leq 5000)$	521 (< 0.1%)	24698 (0.1%)	761513 (3.5%)
Q_6 $Q(/etc//, @size \geq 5000)$	7292 (< 0.1%)	97758 (0.4%)	7015066 (32.9%)
Dataset: XMark:category			
Q_7 $Q(/site/people//interest, 0 \leq @category \leq 50000)$	1910524 (3.1%)	19009723 (31.5%)	6066546 (10.0%)
Q_8 $Q(/site/regions/africa//, 0 \leq @category \leq 50000)$	104500 (0.1%)	1043247 (1.7%)	6066546 (10.0%)
Dataset: Amazon:price			
Q_9 $Q(/CellPhones&Accessories//, 10000 \leq @price \leq 20000)$	2758 (< 0.1%)	291625 (4.3%)	324272 (4.8%)
Q_{10} $Q(/Clothing/Women/*/Sweaters//, 7000 \leq @price \leq 10000)$	239 (< 0.1%)	4654 (< 0.1%)	269936 (4.0%)

space consumption. The type of a node n and its dimension $n.D$ are related. Path nodes typically have a smaller fanout than value nodes. This is to be expected, since paths only contain printable ASCII characters (of which there are about 100), while values span the entire available byte spectrum. Therefore, the most frequent node type for path nodes is type 4, while for value nodes it is type 256, see Figure 8b. Leaf nodes do not partition the data and thus their dimension is set to \perp according to Definition 7. The RCAS index on the ServerFarm:size dataset contains more path than value nodes. This is because in this dataset there are about 9M unique paths as opposed to about 230k unique values. Thus, the values contain fewer discriminative bytes than the paths and can be better compressed by the trie structure.

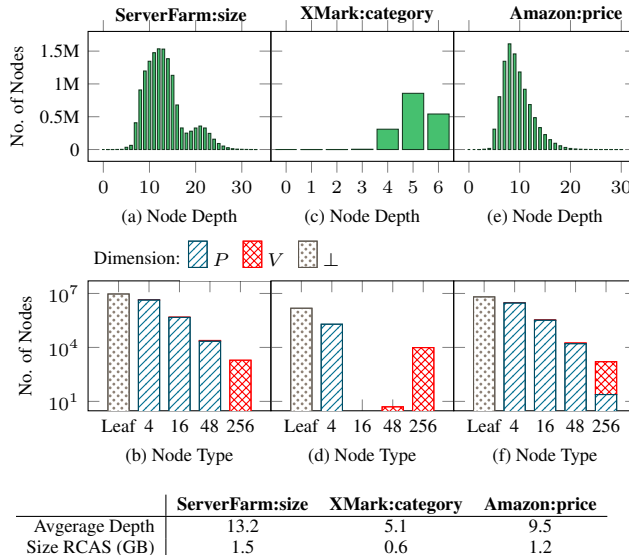


Figure 8: Structure of the RCAS index

Figures 8c and 8d show the same information for dataset XMark:category. The RCAS index is more shallow since there are only 7 unique paths and ca. 390k unique values in a dataset of 60M keys. Thus the number of discriminative path and value bytes is low and the index less deep. Nodes of type 256 are frequent (see Figure 8d) because of the larger number of unique values. While the XMark:category dataset contains 40M more keys than the ServerFarm:size dataset, the RCAS index for the former contains 1.5M nodes as compared to the 14M nodes for the latter. The RCAS in-

dex for the Amazon:price dataset has similar characteristics as the ServerFarm:size dataset, see Figures 8e and 8f.

7.3 Robustness

Table 6 shows a number of typical CAS queries with their path and value predicates. For example, query Q_4 looks for all Makefiles underneath `/usr/share` that have a file size between 1KB and 2KB. In Table 6 we report the selectivity σ of each query as well as path selectivity σ_P and value selectivity σ_V of the queries’ path and value predicates, respectively. The RCAS index avoids large intermediate results that can be produced if an index prioritizes one dimension over the other, or if it independently evaluates and joins the results of the path and value predicates. Query Q_5 , e.g., returns merely 521 matches, but its path and value predicates return intermediate results that are orders of magnitudes larger.

Figures 9a to 9f show that RCAS consistently outperforms its competitors for queries Q_1 to Q_6 from Table 6 on the ServerFarm:size dataset. On these six queries ZO and LW perform similarly as PV, which is indicative for a high “puff-pastry effect” (see Section 3) where one dimension is prioritized over another. In the ServerFarm:size dataset ZO and LW prioritize the path dimension. The reasons are twofold. The first reason is that the `size` attribute is stored as a 64 bit integer since 32 bit integers cannot cope with file sizes above $2^{32} \approx 4.3\text{GB}$. The file sizes in the dataset are heavily skewed towards small files (few bytes or kilo-bytes) and thus have many leading zero-bytes. Many of these most significant bytes do not partition the values. On the other hand, the leading path bytes immediately partition the data: the second path byte is discriminative since the top level of a file system contains folders like `/usr`, `/etc`, `/var`. As a result, ZO and LW fail to interleave at discriminative bytes and these approaches degenerate to the level of PV. The second reason is specific to ZO. To turn variable-length paths into fixed-length strings, ZO maps path labels with a surrogate function and fills shorter paths with trailing zero-bytes to match the length of the longest path (see Section 7.1). We need 3 bytes per label and the deepest path contains 21 labels, thus every path is mapped to a length of 63 bytes and interleaved with the 8 bytes of the values. Many paths in the dataset are shorter than the deepest path and have many trailing zero-bytes. As explained earlier the values (64-bit integers) have many leading zero-bytes, thus the interleaved ZO string orders the relevant path bytes before the relevant value bytes, further pushing ZO towards PV. Let us look more closely at the results of query Q_1 in Figure 9a. VP’s runtime suffers because of the high value selectivity σ_V . XML performs badly because the intermediate result sizes are one to two orders of magnitude larger than the final result size. RCAS with our dynamic interleaving is unaffected by the puff-pastry effect in ZO, LW, and

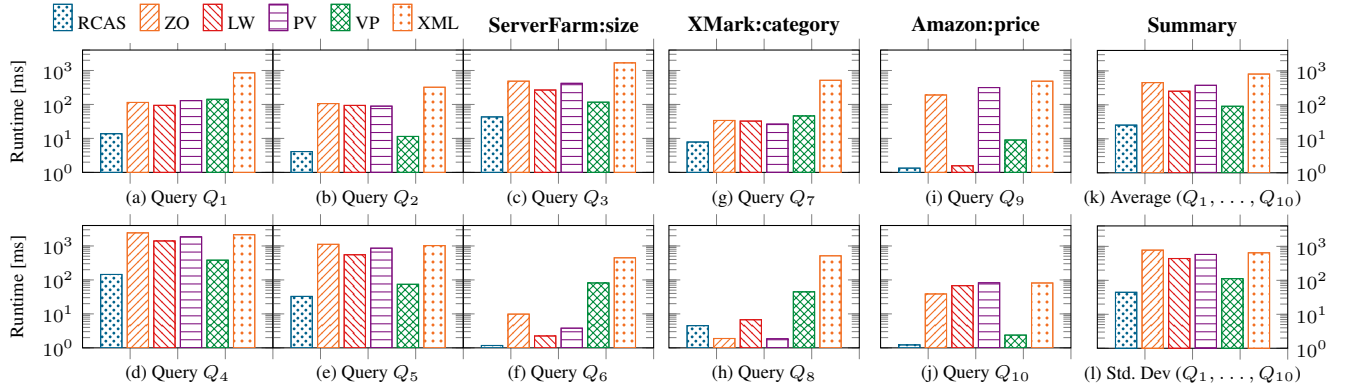


Figure 9: (a)–(j): Runtime measurements for queries Q_1 to Q_{10} in Table 6. (k)–(l): Average and standard deviation for queries Q_1 to Q_{10} .

PV because it only interleaves at discriminative bytes. In RCAS the value selectivity (32%) is counter-balanced by the low path selectivity (2%), thus avoiding VP’s pitfall. Lastly, RCAS does not materialize large intermediate results as XML does.

Queries Q_1 and Q_2 have the same path predicate, but Q_2 ’s value selectivity σ_V is considerably lower. The query performance of ZO, LW, and PV is unaffected by the lower σ_V since σ_P remains unchanged. This is further evidence that ZO and LW prioritize the paths, just like PV. The runtime of VP and XML benefit the most if the value selectivity σ_V drops. RCAS’s runtime still halves with respect to Q_1 and again shows the best overall runtime.

Query Q_3 has the largest individual path and value selectivities, and therefore produces the largest intermediate results. This is the reason for its high query runtime. RCAS has the best performance since the final result size is an order of magnitude smaller than for the individual path and value predicates.

Queries Q_4 and Q_5 look for particular files (`Makefile`, `README`) within large hierarchies. Their low path selectivity σ_P should favor ZO, LW, and PV, but this is not the case. Once Algorithm 4 encounters the descendant axis during query processing, it needs to recursively traverse all children of path nodes ($n.D = P$). Fortunately, value nodes ($n.D = V$) can still be used to prune entire subtrees. Therefore, approaches that alternate between discriminative path and values bytes, like RCAS, can still effectively narrow down the search, even though the descendant axis covers large parts of the index. Instead, approaches that prioritize the paths (PV, ZO, LW) perform badly as they cannot prune subtrees high up during query processing.

Query Q_6 has a very low path selectivity σ_P , but its value selectivity σ_V is high. This is the worst case for VP as it can evaluate the path predicate only after traversing already a large part of the index. This query favors PV, LW, and ZO. Nevertheless, RCAS outperforms all other approaches.

The results for queries Q_7 and Q_8 on the XMark:category dataset are shown in Figures 9g and 9h. The gaps between the various approaches is smaller since the number of unique paths is small (see Section 7.2). As a result, the matching paths are quickly found by ZO, LW, and PV. RCAS answers Q_8 in 4ms in comparison to 2ms for ZO and PV. VP performs worse on query Q_8 because of Q_8 ’s low σ_P and high σ_V .

Query Q_9 on dataset Amazon:price searches for all phones and their accessories priced between \$100 and \$200. Selectivities σ_P and σ_V are roughly 4.5% whereas the total selectivity is two orders of magnitude smaller. Figure 9i confirms that RCAS is the most efficient approach. Query Q_{10} looks for all women’s sweaters priced

between \$70 and \$100. Sweaters exist for various child-categories of category Women, e.g., Clothing, Maternity, etc. Query Q_{10} uses the wildcard $*$ to match all of them.

Figures 9k and 9l show the average runtime and the standard deviation for queries Q_1 to Q_{10} . RCAS is the most robust approach: it has the lowest average runtime and standard deviation.

7.4 Evaluation of Cost Model

This section uses the cost function $\hat{C}(o, h, \phi, \varsigma_P, \varsigma_V)$ from Section 5.3 to estimate the cost of answering a query with RCAS. We explain the required steps for query Q_1 on dataset ServerFarm:size (see Table 6). First, we choose the alternating pattern of discriminative bytes in RCAS’s dynamic interleaving by setting ϕ to (V, P, V, P, \dots) . For determining h and o we consider $|K|$ unique keys. Since each leaf represents a key, there are $o^h = |K|$ leaves. We set h to the average depth of a node in the RCAS index (truncated to the next lower integer) and fanout o to $\sqrt[h]{|K|}$. For dataset ServerFarm:size we have $|K| = 9.3M$ and $h = 13$ (see Table 5 and Figure 8), thus $o = \sqrt[13]{9.3M} = 3.43$. This is consistent with Figure 8a that shows that the most frequent node type in RCAS has a fanout of at most four. Next we look at parameters ς_P and ς_V . In our cost model, a query traverses a constant fraction ς_D of the children on each level of dimension D , corresponding to a selectivity of $\sigma_D = \varsigma_D \cdot \varsigma_D \cdot \dots = \varsigma_D^N$ over all N levels of dimension D . N is the number of discriminative bytes in dimension D . Thus, if a CAS query has a value selectivity of σ_V we set $\varsigma_V = \sqrt[N]{\sigma_V}$. The value selectivity of query Q_1 is $\sigma_V = 32.9\%$ (see Table 6); the number of discriminative value bytes in ϕ is $N = \lceil h/2 \rceil = \lceil 13/2 \rceil = 7$ (we use the ceiling since we start partitioning by V in ϕ), thus $\varsigma_V = \sqrt[7]{0.329} = 0.85$. ς_P is determined likewise and yields $\varsigma_P = \sqrt[13/2]{0.02} = 0.52$ for Q_1 .

We refine this cost model for path predicates containing the descendant axis $//$ or the wildcard $*$ followed by further path steps. In such cases we use the path selectivity of the path predicate up to the first descendant axis or wildcard. For example, for query Q_4 with path predicate `/usr/share//Makefile` and $\sigma_P = 0.03\%$, we use the path predicate `/usr/share//` with a selectivity of $\sigma_P = 44\%$. This is so because the low path selectivity of the original predicate is not representative for the number of nodes that RCAS must traverse. As soon as RCAS hits a descendant axis in the path predicate it can only use the value predicate to prune nodes during the traversal (see Section 6.4).

In Table 7 we compare the estimated cost \hat{C} for the ten queries in Table 6 with the true cost of these queries in RCAS. In addition to the estimated cost \hat{C} and the true cost C , we show the factor

Table 7: Estimated cost \hat{C} and true cost C for queries Q_1 to Q_{10} .

	\hat{C}	C	E		\hat{C}	C	E
Q_1	105 793	83 190	1.27	Q_6	9920	3062	3.24
Q_2	19 157	28 943	1.51	Q_7	34 513	30 365	1.14
Q_3	542 458	273 824	1.98	Q_8	18 856	38 247	2.03
Q_4	710 128	784 068	1.10	Q_9	20 421	4219	4.84
Q_5	111 139	146 124	1.31	Q_{10}	17 993	10 698	1.68

$E = \max(\hat{C}, C) / \min(\hat{C}, C)$ by which the estimate is off. On average the cost model and RCAS are off by only a factor of two.

Figure 10 illustrates that the default values we have chosen for the parameters of \hat{C} yield near optimal results in terms of minimizing the average error \bar{E} for queries Q_1 to Q_{10} . On the x-axis, we plot the deviation from the default value of a parameter. The values for o and h are spot on. We overestimate the true path and value selectivities by a small margin; decreasing Δ_{SP} and Δ_{SV} by 0.04 improves the error marginally.

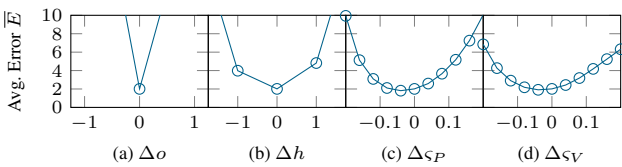


Figure 10: Calibrating the cost model

7.5 Space Consumption and Scalability

Figure 11 illustrates the space consumption of the indexes for our datasets. RCAS, ZO, LW, PV, and VP all use the same underlying trie structure and have similar space requirements. The XMark:category dataset can be compressed more effectively using tries because the number of unique paths and values is low (see Section 7.2) and common prefixes need to be stored only once. The trie indexes on Amazon:price do not compress the data as well as on the other two datasets since the lengthy titles of products do not share long common prefixes. The XML index needs to maintain two structures, a DataGuide and a B+ tree. Consequently, its space consumption is higher. In addition, prefixes are not compressed as effectively in a B+ tree as they are in a trie.

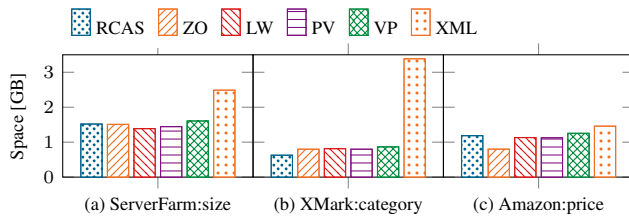


Figure 11: Space consumption

In Figure 12 we analyze the scalability of the indexes in terms of their space consumption and bulk-loading time as we increase the number of (k, r) pairs to 100M. We scale the ServerFarm:size dataset as needed to reach a certain number of (k, r) pairs. The space consumption (Figure 12a) and the index bulk-loading time (Figure 12b) are linear in the number of keys. The small drop for RCAS, ZO, LW, PV, and VP in Figure 12a is due to their trie structure. These indexes compress the keys more efficiently when we scale the dataset from originally 21M keys to 100M keys (we do so by duplicating keys). They store the path $k.P$ and value $k.V$ only

once for pairs (k, r_i) and (k, r_j) with the same key k . Figure 12b confirms that the time complexity of Algorithm 3 to bulk-load the RCAS index is linear in the number of keys (see Lemma 3). Bulk-loading RCAS is a factor of two slower than bulk-loading indexes for static interleavings, but a factor of two faster than bulk-loading the XML index. While RCAS takes longer to create the index it offers orders of magnitude better query performance as shown before. Figure 12 shows that the RCAS index for 100M keys requires 2GB of memory and can be bulk-loaded in less than 5 minutes.

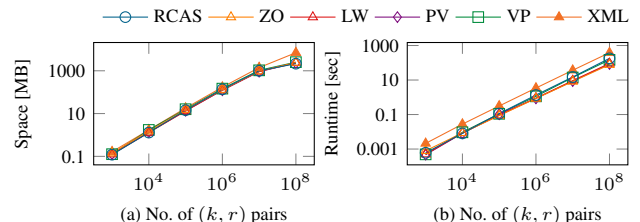


Figure 12: Space consumption and bulk-loading time

7.6 Summary

We conclude with a summary of the key findings of our experimental evaluation. First, RCAS shows the most robust query performance for a wide set of CAS queries with varying selectivities: it exhibits the most stable runtime in terms of average and standard deviation, outperforming other state-of-the-art approaches by up to two orders of magnitude. Second, our cost model yields a good estimate for the true cost of a CAS query on the RCAS index. Third, because of the trie-based structure the RCAS index consumes less space than its competitors, requiring only a third of the space used by a B+ tree-based approach. The space consumption and bulk-loading time are linear in the number of keys, allowing it to scale to a large number of keys.

8. CONCLUSION AND OUTLOOK

We propose the Robust Content-and-Structure (RCAS) index for semi-structured hierarchical data, offering a well-balanced integration of paths and values in a single index. Our scheme avoids prioritizing a particular dimension (paths or values), making the index robust against queries with high individual selectivities producing large intermediate results and a small final result. We achieve this by developing a novel dynamic interleaving scheme that exploits the properties of path and value attributes. Specifically, we interleave paths and values at their *discriminative bytes*, which allows our index to adapt to a given data distribution. In addition to proving important theoretical properties, such as the monotonicity of discriminative bytes and robustness, we show in our experimental evaluation impressive gains: utilizing dynamic interleaving our RCAS index outperforms state-of-the-art approaches by up to two orders of magnitudes on real-world and synthetic datasets.

Future work points into several directions. We plan to apply RCAS on the largest archive of software source code, the Software Heritage Dataset [10, 34]. On the technical side we are working on supporting incremental insertions and deletions in the RCAS index. It would also be interesting to explore a disk-based RCAS index based on a disk-based trie [3]. Further, we consider making path predicates more expressive by, e.g., allowing arbitrary regular expressions as studied by Baeza-Yates et al. [5]. On the theoretical side it would be interesting to investigate the length of the dynamic interleavings for different data distributions.

9. REFERENCES

- [1] S. Alsubaiee et al. Asterixdb: A scalable, open source bdms. *PVLDB*, 7(14):1905–1916, 2014.
- [2] Apache. Apache Jackrabbit Oak. <https://jackrabbit.apache.org/oak/>, 2020. [Online; accessed May 2020].
- [3] N. Askitis and J. Zobel. B-tries for disk-based string management. *VLDB J.*, 18(1):157–179, 2009.
- [4] R. Baca, M. Krátký, I. Holubová, M. Necaský, T. Skopal, M. Svoboda, and S. Sakr. Structural XML query processing. *ACM Comput. Surv.*, 50(5):64:1–64:41, 2017.
- [5] R. A. Baeza-Yates and G. H. Gonnet. Fast text searching for regular expressions or automaton searching on tries. *J. ACM*, 43(6):915–936, 1996.
- [6] R. Binna, E. Zangerle, M. Pichl, G. Specht, and V. Leis. Hot: A height optimized trie index for main-memory database systems. In *SIGMOD*, pages 521–534, 2018.
- [7] R. Brunel, J. Finis, G. Franz, N. May, A. Kemper, T. Neumann, and F. Färber. Supporting hierarchical data in SAP HANA. In *ICDE*, pages 1280–1291, 2015.
- [8] B. F. Cooper, N. Sample, M. J. Franklin, G. R. Hjaltason, and M. Shadmon. A fast index for semistructured data. In *VLDB*, pages 341–350, 2001.
- [9] CouchDB. CouchDB. <http://couchdb.apache.org/>, 2020. [Online; accessed May 2020].
- [10] R. Di Cosmo and S. Zacchiroli. Software heritage: Why and how to preserve software source code. In *iPRES*, 2017.
- [11] J. Finis, R. Brunel, A. Kemper, T. Neumann, F. Färber, and N. May. Deltani: an efficient labeling scheme for versioned hierarchical data. In *SIGMOD*, pages 905–916, 2013.
- [12] J. Finis, R. Brunel, A. Kemper, T. Neumann, N. May, and F. Färber. Indexing highly dynamic hierarchical data. *PVLDB*, 8(10):986–997, 2015.
- [13] J. Finis, R. Brunel, A. Kemper, T. Neumann, N. May, and F. Färber. Order indexes: supporting highly dynamic hierarchical data in relational main-memory database systems. *VLDB J.*, 26(1):55–80, 2017.
- [14] D. Florescu and G. Fourny. JSONiq: The history of a query language. *IEEE Internet Computing*, 17(5):86–90, 2013.
- [15] R. Goldman and J. Widom. Dataguides: Enabling query formulation and optimization in semistructured databases. In *VLDB*, pages 436–445, 1997.
- [16] G. Graefe. Robust query processing. In *ICDE*, page 1361, April 2011.
- [17] G. Graefe, W. Guy, H. A. Kuno, and G. N. Paulley. Robust query processing (Dagstuhl Seminar 12321). *Dagstuhl Reports*, 2(8):1–15, 2012.
- [18] R. He and J. J. McAuley. Ups and downs: Modeling the visual evolution of fashion trends with one-class collaborative filtering. In *WWW*, pages 507–517, 2016.
- [19] H. Katz, D. Chamberlin, M. Kay, P. Wadler, and D. Draper. *XQuery from the Experts: A Guide to the W3C XML Query Language*. Addison-Wesley, Boston, 2003.
- [20] R. Kaushik, R. Krishnamurthy, J. F. Naughton, and R. Ramakrishnan. On the integration of structure indexes and inverted lists. In *SIGMOD*, pages 779–790, 2004.
- [21] V. Leis, A. Kemper, and T. Neumann. The adaptive radix tree: Artful indexing for main-memory databases. In *ICDE*, pages 38–49, 2013.
- [22] J. J. Levandoski, D. B. Lomet, and S. Sengupta. The bw-tree: A b-tree for new hardware platforms. In *ICDE*, 2013.
- [23] H. Li, S. A. Aghili, D. Agrawal, and A. El Abbadi. FLUX: content and structure matching of xpath queries with range predicates. In *XSym*, pages 61–76, 2006.
- [24] V. Markl. *MISTRAL: Processing Relational Queries using a Multidimensional Access Technique*. PhD thesis, Technical University of Munich, 1999.
- [25] C. Mathis, T. Härdter, K. Schmidt, and S. Bächle. XML indexing and storage: fulfilling the wish list. *Computer Science - R&D*, 30(1), 2015.
- [26] T. Milo and D. Suciu. Index structures for path expressions. In *ICDT*, pages 277–295, 1999.
- [27] MongoDB. MongoDB Indexing. <https://docs.mongodb.com/v4.0/indexes/>, 2020. [Online; accessed May 2020].
- [28] D. R. Morrison. PATRICIA - practical algorithm to retrieve information coded in alphanumeric. *J. ACM*, 15(4):514–534, 1968.
- [29] G. Morton. A computer oriented geodetic data base; and a new technique in file sequencing. Technical report, IBM Ltd., 1966.
- [30] B. G. Nickerson and Q. Shi. On k-d range search with patricia tries. *SIAM J. Comput.*, 37(5):1373–1386, 2008.
- [31] S. Nishimura and H. Yokota. QUILTS: multidimensional data partitioning framework based on query-aware and skew-tolerant space-filling curves. In *SIGMOD*, pages 1525–1537, 2017.
- [32] P. E. O’Neil, E. J. O’Neil, S. Pal, I. Cseri, G. Schaller, and N. Westbury. Orddpaths: Insert-friendly XML node labels. In *SIGMOD*, pages 903–908, 2004.
- [33] J. A. Orenstein and T. H. Merrett. A class of data structures for associative searching. In *PODS*, pages 181–190, 1984.
- [34] A. Pietri, D. Spinellis, and S. Zacchiroli. The software heritage graph dataset: public software development under one roof. In *MSR*, pages 138–142, 2019.
- [35] F. Ramsak, V. Markl, R. Fenk, M. Zirkel, K. Elhardt, and R. Bayer. Integrating the ub-tree into a database system kernel. In *VLDB*, pages 263–272, 2000.
- [36] H. Samet. *Foundations of multidimensional and metric data structures*. Morgan Kaufmann series in data management systems. Academic Press, 2006.
- [37] A. Schmidt, F. Waas, M. L. Kersten, M. J. Carey, I. Manolescu, and R. Busse. Xmark: A benchmark for XML data management. In *VLDB*, pages 974–985, 2002.
- [38] A. Shanbhag, A. Jindal, S. Madden, J. Quiane, and A. J. Elmore. A robust partitioning scheme for ad-hoc query workloads. In *SoCC*, pages 229–241, 2017.
- [39] D. Shukla et al. Schema-agnostic indexing with azure DocumentDB. *PVLDB*, 8(12):1668–1679, 2015.
- [40] K. Wellenzohn, M. H. Böhlen, and S. Helmer. Dynamic interleaving of content and structure for robust indexing of semi-structured hierarchical data (extended version). Technical report, CoRR, 2020. <https://arxiv.org/pdf/2006.05134.pdf>.
- [41] H. Zhang, H. Lim, V. Leis, D. G. Andersen, M. Kaminsky, K. Keeton, and A. Pavlo. Surf: Practical range query filtering with fast succinct tries. In *SIGMOD*, pages 323–336, 2018.